Bulletin of Electrical Engineering and Informatics
Vol. 13, No. 3, June 2024, pp. 1602~1612
ISSN: 2302-9285, DOI: 10.11591/eei.v13i3.6658

Design of a novel compact low specific absorption rate multiple input multiple output antenna for 5G sub-6 GHz terminals

Abdelhadi Ennajih[1], Azzeddine Sardi[2], Youssef Mouzouna[1], Mohamed Sadik[1], Ahmed Errkik[2]
[1]NEST Research Group, Engineering Research Laboratory (LRI. Lab), Department of Electrical Engineering, National Higher School of Electricity and Mechanics, Hassan II University, Casablanca, Morocco
[2]Laboratory of Mechanics, Computing, Electronics, and Telecommunications (LMIET), Faculty of Science and Technology, Hassan I University, Settat, Morocco

Article Info

Article history:

Received May 6, 2023
Revised Sep 1, 2023
Accepted Sep 11, 2023

Keywords:

5G technology
Metamaterial
Multiple input multiple output antenna
Smartphone
Specific absorption rate

ABSTRACT

This investigation presents a new design and analysis of a fourteen elements massive multiple input multiple output (MIMO) compact low specific absorption rate (SAR) antenna system for 5G and beyond terminals. The MIMO antennas are realized for sub-6 GHz LTE-band 46 (5.1-5.8 GHz) long-term evolution 5G wireless communication services. The proposed antenna system is designed on an FR-4 dielectric constant 4.3 substrate consisting of the main board and four sideboards. The radiating elements are developed on the sideboards consisting of a monopole antenna and two metamaterial unit cells, as well as the feed line is designed on the principal board. The overall volume of the proposed structure is 150×80×7.5 mm. Through the use of the metamaterial unit cells, the proposed antennas have been arranged in close proximity without developing a strong mutual coupling. The results obtained were very important in terms of impedance matching, isolation among the antennas, and good gain. Even, the SAR analysis at the operating frequency band of 5.5 GHz proves that the proposed MIMO antenna system satisfies safety standards set for human exposure at the international level. Therefore, the proposed massive MIMO antenna structure is a potential solution for future communication applications.

Corresponding Author:

Abdelhadi Ennajih
NEST Research Group, Engineering Research Laboratory, Department of Electrical Engineering
National Higher School of Electricity and Mechanics, Hassan II University
Casablanca, Morocco
Email: a.ennajih@ensem.ac.ma

1. INTRODUCTION

Telecommunications technology has come a long way in the last decade. In fact, the quality of signal transmission has evolved from 1th generation (1G) to 4th generation (4G). Each new technological device increases throughput and leads to the expectation of faster transmission speeds [1]. Despite its many advantages, 4G technology has some drawbacks related to lack of coverage, network connection failures, and channel saturation. The rapid development of connected objects and devices means that 4G technology will not be able to satisfy the emerging trends. Therefore, an upgrade to the 5th generation (5G) has become necessary [2].

As 5G and beyond (5G/B) become more widely adopted and standardized, research into related technologies is intensifying to deliver faster speeds, lower costs, and higher gains, with future generations of 5G smartphones requiring better link reliability and data rates around 1000 times faster than 4G. The 5G

operates in two key frequency ranges to provide broad coverage and cover all use cases. These two ranges are the sub-6 GHz range and the millimeter wave range. For the sub-6 GHz range, several frequency bands have been proposed to meet the bandwidth demands of the 5G next-generation smartphone, such as the LTE-band 43/42 (from 3.4 GHz to 3.8 GHz), the LTE-band 46 (from 5.15 GHz to 5.925 GHz), and the EU multi-band (5.9 GHz to 6.4 GHz) allocated by the European Union [3]. Due to the use of the new 5G LTE 46 band, exchanging or viewing files of all kinds, including huge files such as videos, is almost instantaneous [1], [4].

The antenna is an essential element of the mobile communication system to guarantee the coverage of the communication network. Consequently, using a single antenna cannot ensure the requirements of 5G technology, so the use of a multiple input multiple output (MIMO) system is necessary. Low-order MIMO antenna systems, such as 2×2 and 4×4, are quite popular for the current generation of 4G mobile phones [5]–[7]. However, these specifications cannot be met using low-order MIMO antenna systems. Therefore, switching to high-order MIMO antenna systems is a suitable solution, but the use of multiple antennas will reduce the effect of the user's hands blocking certain antenna elements and degrading link performance.

Due to the limited dimensions of mobile phones, integrating several antennas in a small space is challenging. Indeed, the insertion of many antennas can lead to interference between the MIMO antenna system elements which is due to mutual coupling. To overcome these challenges, many different designs of MIMO antennas have recently been proposed for 5G mobile phones. However, these MIMO antennas either suffer from the low order of the integrated antennas or take up a tremendous amount of space on the phone's main board [8]–[13]. The main objective of this work is the development of a new MIMO system that integrates more elements that present a good performance in terms of reduced size, low mutual coupling across the MIMO elements with a very low specific absorption rate to protect the user from electromagnetic radiation in compliance with IEEE standards. To this end, in this study, we propose to design a metamaterial-based MIMO system starting with the design and extraction of the magnetic and electrical parameters of a unitary metamaterial cell, then proceed to the design of a single antenna and the implementation of a MIMO structure comprised of multiple antenna elements, the design steps are described in detail in the next section.

2. DESIGN OF MIMO ANTENNA

2.1. Proposed unit cell

Metamaterials are materials that possess a homogeneous composition that is not found in ordinary materials, such as negative permittivity or permeability, or both [14]. In the microwave field, metamaterials are used either to miniaturize the size of passive circuits or antennas, for performance enhancement or to reduce the mutual coupling between antenna array elements [15]–[19]. In this work, the proposed metamaterial unit cell is used for both purposes: minimizing the size of antennas and reducing the interference between MIMO antenna elements. Its structure consists of a rectangular-split-ring-resonator (RSRR) designed on one side of the FR-4subsstrate with a dielectric constant of 4.3 and thickness of h=1.6 mm. Figure 1(a) illustrates the proposed RSRR in a transverse electric and magnetic (TEM) box, where the electric and magnetic walls are defined along the x and z axes, respectively, and the waveguide ports are defined along the y-axis. The dimensions of the RSRR are adjusted to obtain a negative permeability around the LTE 46 band. The electrical and magnetic parameters of the unit cell are extracted from S-parameters and show that the RSRR has a negative permittivity around the desired frequency band, as illustrated in Figure 1(b).

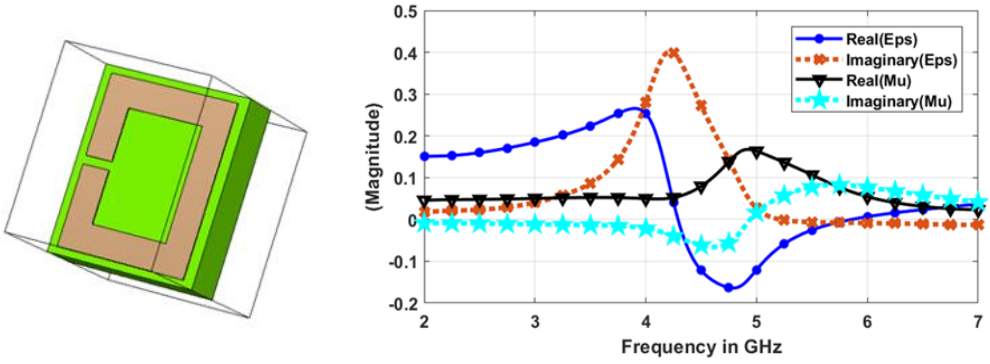

(a) (b)

Figure 1. Proposed metamaterial unit cell; (a) geometry and (b) electrical and magnetic parameters

2.2. Single antenna element

After designing the metamaterial unit cell in the previous section, this section discusses the geometry of the proposed single antenna, which comprises a monopole antenna in the form of a transmission line modeled on the bilateral substrate and fed by a second transmission line designed on the main substrate. The RSRR metamaterial cell that has been designed in the first section has been placed alongside the monopole antenna to improve impedance matching in order to make the antenna operate around the desired frequency. Figures 2(a)-(c) show the various stages involved in designing the final structure of the single antenna and Table 1 shows the parameter values.

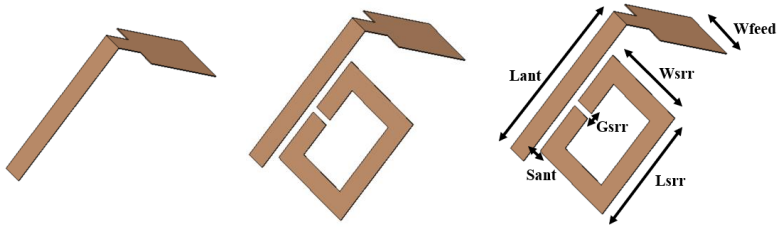

Figure 2. The proposed antenna geometry; (a) stage 1, (b) stage 2, and (c) dimensions

Table 1. Parameters of the single antenna

Variable	Value (mm)	Variable	Value (mm)
Lant	7.5	Want	1
Lsrr	6	Wsrr	4.8
Lfeed	6	Gsrr	0.3
Wfeed	2.75	Sant	0.4

2.3. MIMO antenna system

In order to design a MIMO system that consists of fourteen elements, ten of them are mounted on bilateral substrates sized 7.5×150 mm² along the x-axis with a separation distance between the different elements of 13.6 mm. A second RSRR metamaterial cell of about the same size as the first has been added to separate the different elements of the MIMO system in order to reduce mutual coupling as depicted in Figures 3(a) and (b). Important results were obtained using a parametric study of the space separating the antenna and the RSRR cell. Having the antennas arranged in parallel provides two electric fields 90° out of phase and leads to dual polarization. The dimension of the main substrate is 80×150 mm, while the dimensions of the bilateral substrates are 7.5×80 mm for the first substrate and 7.5×150 mm for the second substrate. The complete structure of the proposed MIMO system is presented in Figure 3(c). To illustrate the effect of the metamaterial cells, the MIMO system was simulated with and without the RSRR cell for two elements. Figure 4 shows the computed S-parameters, as observed, positive results are obtained by adding the RSRR cells in terms of reflection coefficient and isolation at the operating band.

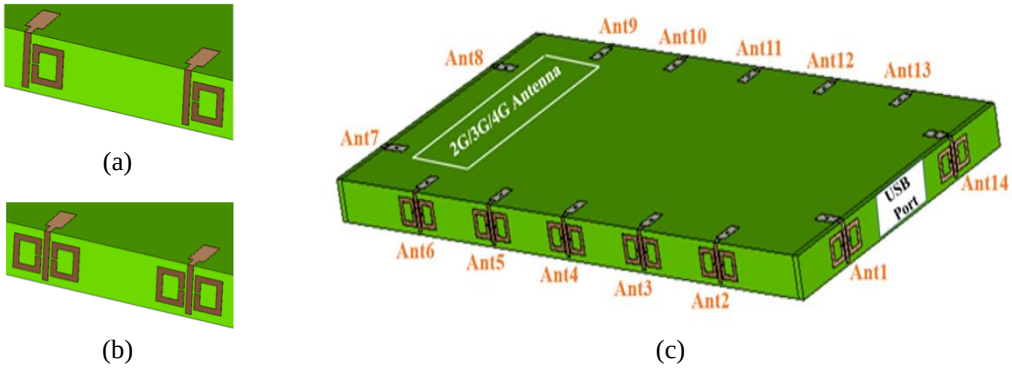

Figure 3. General view of 5G MIMO antenna; (a) two MIMO antenna elements with one unit cell, (b) two MIMO antenna elements with two-unit cells, and (c) the complete MIMO antenna structure

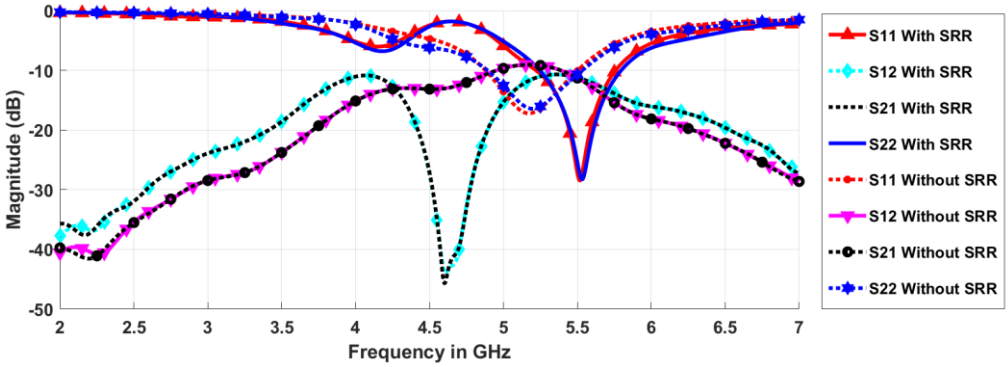

Figure 4. The computed S-parameters of 5G MIMO antenna with and without unit cell

3. RESULTS AND DISCUSSION

3.1. S-parameters and radiation patterns

Figures 5(a) and (b) depict the response of the proposed antenna system in terms of return loss. Due to the symmetry of the MIMO system and the similarity of all antennas in design, the values of the reflection coefficients remain approximately the same. Therefore, only one side will be presented. It can be clearly seen that the amplitude of the return loss for all antennas is less than -25 dB. The radiation pattern performance was evaluated for Ant1 (also corresponding to Ant7, Ant8, and, Ant14), Ant2 (also corresponding to Ant6, Ant9, and, Ant13), Ant3 (also corresponding to Ant5, Ant10, and, Ant12), and Ant4 (also corresponding to Ant11) at the center frequency of 5.5 for two main planes phi=0° and phi=90°, which correspond respectively to the vertical and the orthogonal planes, as noticed in Figures 6(a)-(d). It is possible to observe that both planes E and H are approximately unidirectional for all antennas.

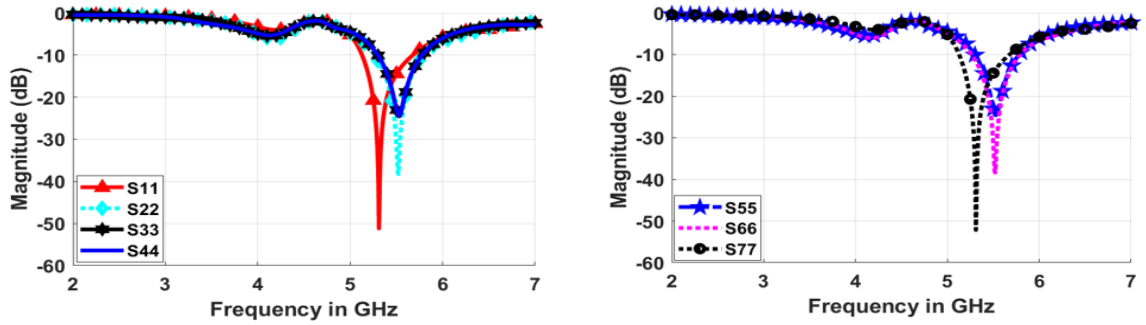

(a) (b)

Figure 5. Simulated reflection coefficient; (a) S11, S22, S33, and S44 and (b) S55, S66, and S77

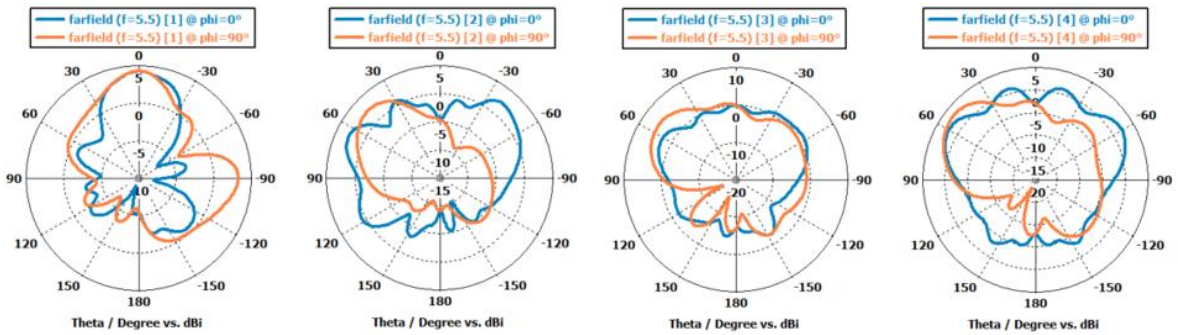

(a) (b) (c) (d)

Figure 6. The radiation patterns of the antennas; (a) Ant1, (b) Ant2, (c) Ant3, and (d) Ant4

The isolation of the MIMO antenna system can be evaluated by the envelope-correlation coefficient (ECC), which measures the independence of the radiation patterns of the MIMO system. Several approaches to calculating the correlation coefficient (ρij) between two antennas, "Ant i" and "Ant j", are discussed in [20]. The coefficient (ρij) can be evaluated from the radiation patterns using the following expressions:

$$\rho_{ij} = \left| \frac{\int_0^{2\pi}\int_0^{\pi}\left(CPR.E_{\theta i}E_{\theta j}^{*}.P_{\theta}+CPR.E_{\varphi i}E_{\varphi j}^{*}.P_{\varphi}\right)sin(\theta)d\theta d\varphi}{\sqrt{\Pi_{k=i,j}\int_0^{2\pi}\int_0^{\pi}\left(CPR.E_{\theta k}E_{\theta k}^{*}.P_{\theta}+CPR.E_{\varphi k}E_{\varphi k}^{*}.P_{\varphi}\right)sin(\theta)d\theta d\varphi}} \right|^2 \quad (1)$$

Where: P_{φ} and P_{θ} satisfies the following conditions:

$$P_{\varphi}\, sin(\theta)d\theta d\varphi = P_{\theta}\, sin(\theta)d\theta d\varphi \quad (2)$$

P_{φ} and P_{θ} represent the environment propagation power spectrum. Cross-polarization ratio (CPR). $E_{\varphi(i,j)}$ and $E_{\theta(i,j)}$ represent the electric field components of antenna elements i and j, (here) while θ and φ indicate respectively the vertical and horizontal polarisation. Generally, the ECC must be close to (zero) 0 for perfect isolation and must not exceed 0.5 [21], which is reached by the proposed system over the whole band as can be seen in Figures 7(a) and (b).

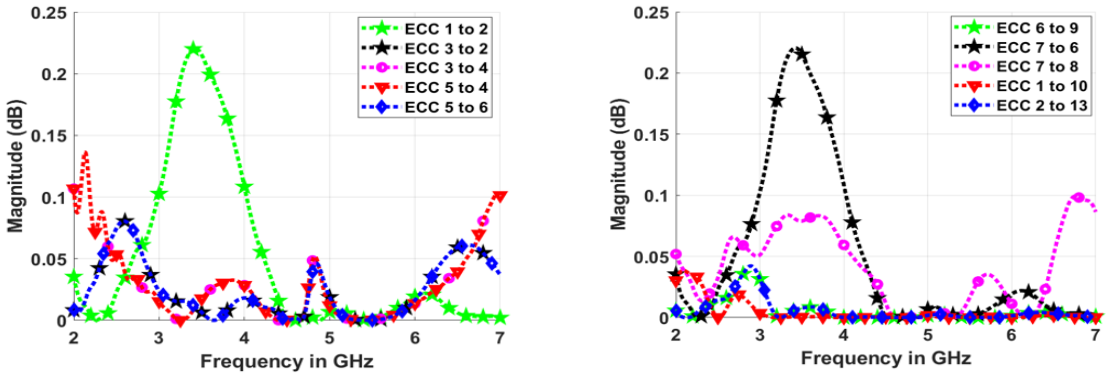

(a) (b)

Figure 7. Simulated ECC; (a) ECC 1 to 2, ECC 3 to 2, ECC 3 to 4, ECC 5 to 4, and ECC 5 to 6 and (b) ECC6 to 9, ECC 7 to 6, ECC 7 to 8, ECC 1 to 10, and ECC 2 to 13

Diversity gain (DG) is also a very important characteristic to consider in MIMO antennas and can be evaluated from S-parameters using (3):

$$DG = 10\sqrt{1-\left(\frac{\left|S_{1,1}^{*}S_{2,1}+S_{1,2}^{*}S_{2,2}\right|^2}{\left(1-|S_{2,1}|^2-|S_{2,2}|^2\right)^{*}\left(1-|S_{1,1}|^2-|S_{1,2}|^2\right)}\right)^2} \quad (3)$$

For the proposed system, the standard DG value that must be met so that the reduction in transmitted power will not have a major effect on transmission quality or MIMO performance is 10 dB or close to it. For the developped system, and as dipected in Figures 8(a) and (b), the DG value is close to 10 for the whole operating bandwidth, which satisfies the norm's criteria. The MIMO antenna system total efficiency is evaluated using (4):

$$Efficiency = 100 * \left(\frac{Gain}{Directivity}\right) \quad (4)$$

As observed in Figures 9(a) and (b), the total efficiency is between 80% and 98% at the operating frequency. These results in terms of reflection coefficient and ECC confirm that the elements of the MIMO system have excellent impedance matching and are perfectly arranged, ensuring that no antenna affects the performance of neighboring elements. The presented antenna effectiveness can also be evaluated through

surface of current distribution. As seen in Figure 10, the highest current is noticed near to the metamaterial cells.

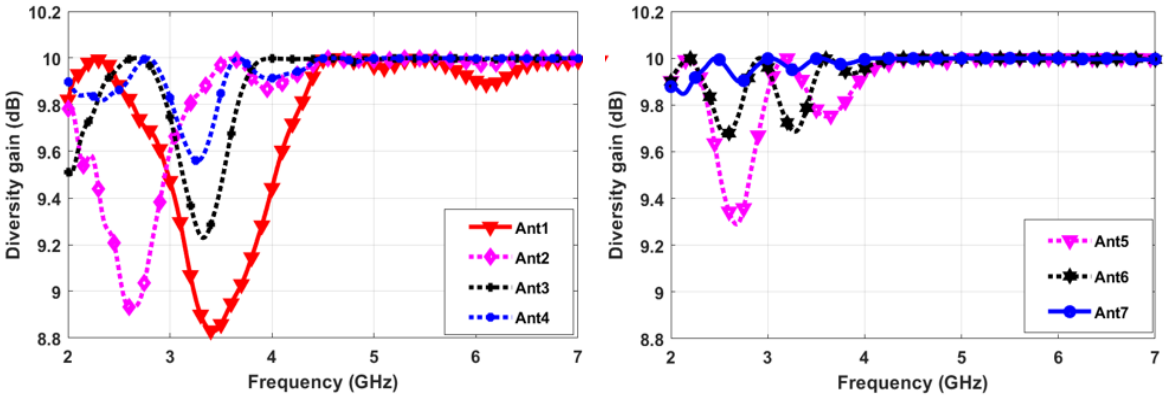

Figure 8. Diversity gains of the proposed antenna for; (a) Antenna1, Antenna2, and Antenna3 and (b) Antenna5, Antenna6, and Antenna7

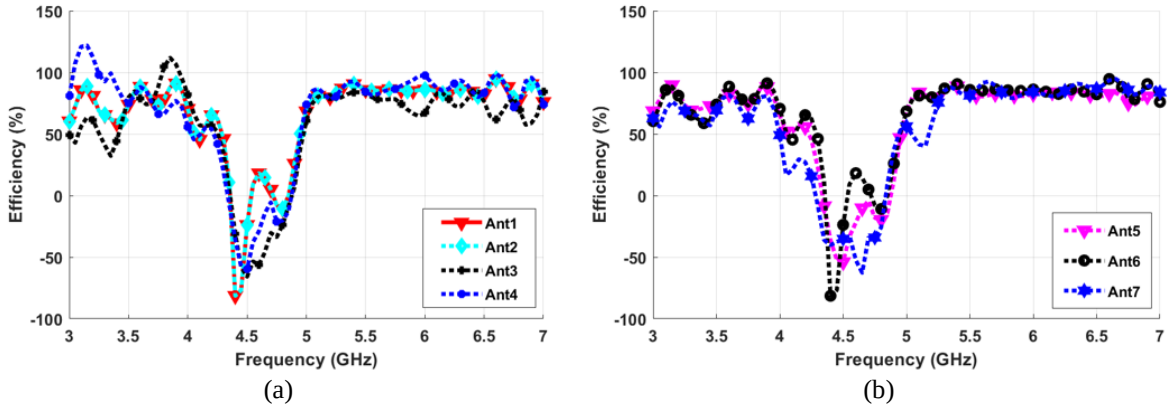

Figure 9. Total efficiency of the proposed antenna for; (a) Antenna1, Antenna2, and Antenna3 and (b) Antenna5, Antenna6, and Antenna7

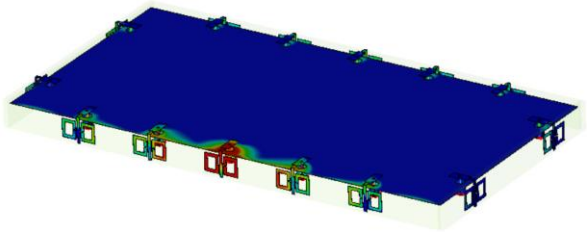

Figure 10. Surface current distribution

3.2. Impact of human's hand

The influence of the grip of the human hand is analyzed in this section. A handheld mobile phone is used in two different scenarios, specifically the calling scenario using a single hand and the gaming scenario using two hands. A representation of the two scenarios involving handheld mobile phone is shown in Figure 11. As shown in Figure 11(a), 8 antennas are not in contact with the operator's hand and, therefore, will not be affected by (the operator's hand) it. However, the other six antennas are close to the user's hand

and, therefore, probably can be affected. In the second situation, as illustrated in Figure 11(b), 8 antennas are in contact with the user's hand.

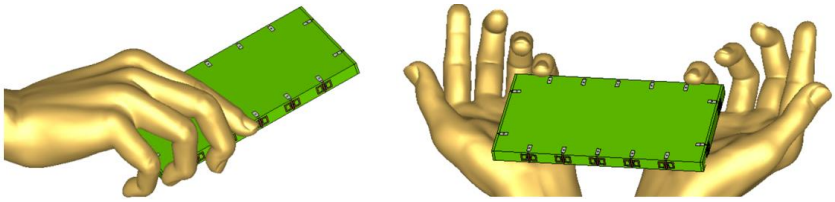

(a) (b)

Figure 11. Hand held mobile phone representation; (a) calling mode and (b) gaming mode

The influence of the single-hand mode on the antenna effeciency, such as the reflection coefficient (S11) and the ECC are also dicussed in this paragraph. The calculated reflection coefficient of Ant2, Ant3, and Ant4 is presented in Figure 12. As depicted in this figure, there is a minor variation of the reflection coefficient for these antennas, which are in contact with the user's hand. However, the return loss remains below -25 dB, which is a good impedance matching. Nevertheless, for the other antennas, the user's hand has no effect on the reflection coefficient.

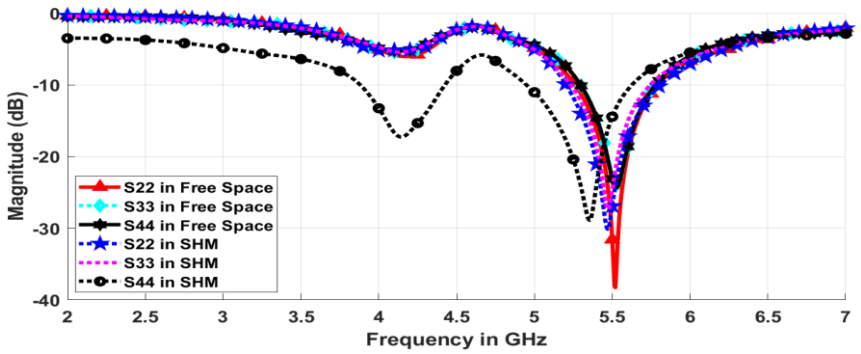

Figure 12. Comparaison of the reflection coefficient in free space and in single hand mode

The mutual coupling or the isolation between the antennas was also evaluated through the ECC and Figures 13(a) and (b) show the obtained results. The computed results show that the ECC is under 0.22 dB. These results conclude that the proposed antenna can be considered satisfactory and present a robust design for innovative 5G smartphones.

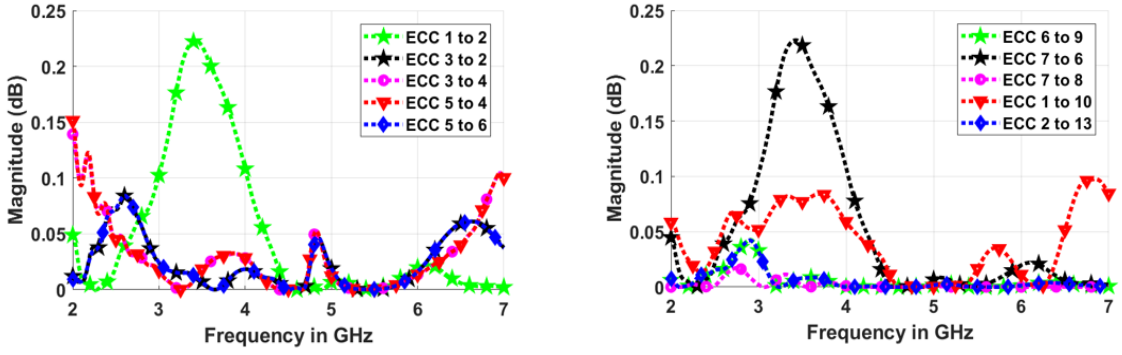

(a) (b)

Figure 13. Simulated ECC in single hand mode; (a) ECC 1 to 2, ECC 3 to 2, ECC 3 to 4, ECC 5 to 4, and ECC 5 to 6 and (b) ECC6 to 9, ECC 7 to 6, ECC 7 to 8, ECC 1 to 10, and ECC 2 to 13

3.3. SAR analysis

The SAR is a prime factor in the measurement of the highest absorption rate by human tissue when comes into contact with radiofrequency electromagnetic field. According to the IEEE standards association, the SAR limit value specified in IEEEC95.1: 1999 is 1.6 W/Kg for an average mass of 1 g while that specified in IEEE C95.1: 2019 must not exceed 2 W/Kg for a typical mass of 10 g. In this study, a 3D model of the human head was used to analyse the absorption rate value of the designed MIMO antenna system. Figure 14(a) illustrates the human head model with the proposed MIMO system.The SAR can be calculated from the electric field E, the human tissue mass density ρ and, conductivity σ, as (5) [22]:

$$SAR = \frac{\sigma |E|^2}{\rho} \quad (5)$$

The proposed MIMO antenna system was placed at 5 mm from the human head model, and the computed SAR distribution using a different number of antennas is illustrated in Figures 14(b)-(d). As can be seen in the figure, the highest SAR value for 10 g averaging mass tissue for the tree cases is under 0.288 W/Kg. This is due to the radiating elements of the antennas which are mounted on bilateral substrates and thus their radiation will be directed outwards from the human body during a call. Even with 14 elements, the SAR remains unchanged because the MIMO antennas are not coupled to each other, which confirms that this MIMO antenna system respects the IEEE standard.

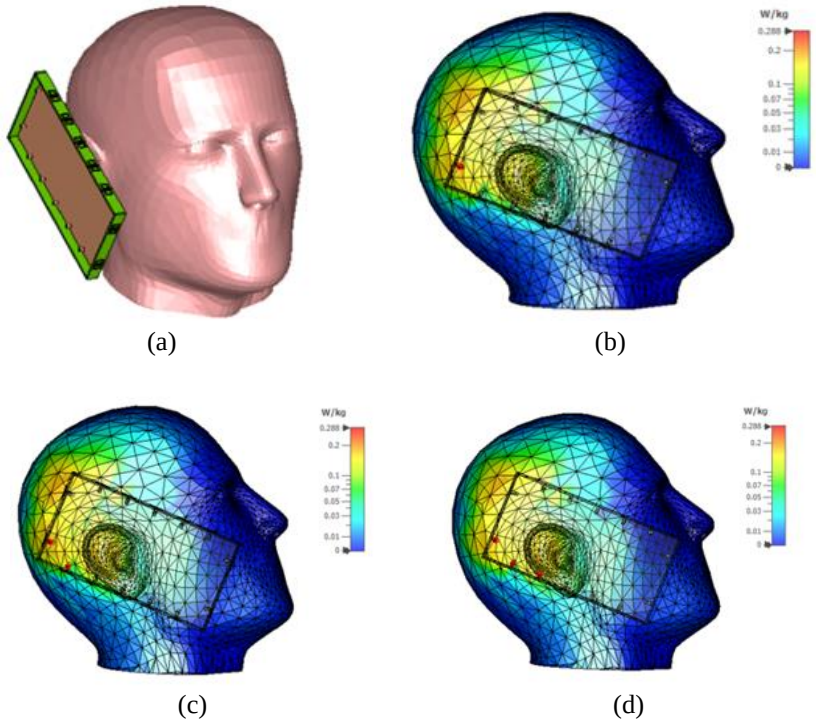

Figure 14. Human head; (a) 3D model of SAR calculation, (b) SAR distribution using one antenna, (c) SAR distribution using two antennas, and (d) SAR distribution using three antennas

3.4. Comparison of the designed MIMO antenna with other works

The performance of the proposed MIMO system has been compared with other works published recently, in terms of dimensions, correlation coefficient, SAR, and resonant bandwidth. As depicted in Table 2, the proposed structure has a very low SAR, below 0.288 W/Kg, compared to the only references [22], [23] that were studied and obtained acceptable values, but slightly higher than the results obtained in our work. Furthermore, the analysis of the interdependency between the different elements of the system shows that the envelope correlation coefficient, which assesses the dependency and grows with the number of components in the MIMO system, is lower than those presented in the table, except to [24], where only two antennas are used. Given that the proposed system comprises fourteen elements and that most previous works propose only eight. Another feature of the proposed system is its efficiency, which can be as high as 90%.

The results obtained show significant values, indicating that the proposed MIMO system is a good solution for 5G mobile phones.

Table 2. Performance comparison of proposed MIMO antenna system with published works

Ref.	Main board dimensions (mm²)	Num. of antennas	Efficiency (%)	Frequency bands (GHz)	SAR (W/Kg)	ECC
[22]	150×75	8	65-80	3.4-4.4	<2.1	<0.05
[23]	110×75	6	71	5.63-5.85/26.19-30.25	<0.59	<0.05
[24]	100×60	2	75	2.3-3.0/4.7-5.9	Not provided	<0.0058
[25]	150×75	8	58-62/68-74	3.4-3.6/5.1–5.7	Not provided	<0.02
[26]	150×75	8	60-65/58-70	3.4-3.6/5.1-5.9	Not provided	<0.02
[27]	150×80	8	50–92	3.3-5.82	Not provided	<0.04
[28]	140×70	8	49–60/62–79	3.4-3.6/5.4-5.6	Not provided	<0.10
[29]	150×80	18	87-93	3.3-3.8	Not provided	<0.10
Proposed	150×80	14	70-90	5.2-5.8	<0.288	<0.01

4. CONCLUSION

This paper describes the design of a fourteen-element MIMO antenna based on metamaterial cells for 5G mobile phone applications at sub-6 GHz operating in the LTE 47 frequency band. The proposed structure is mounted on two-side substrates to receive dual polarized waves and reduce the absorption of the electromagnetic field by the user's biological tissues. The performance and fundamental features of the MIMO system are discussed, and satisfactory results are achieved in terms of gain, impedance matching, among antenna elements, and, the number of elements arranged in a single board. From the configuration of the MIMO system, the mutual coupling among antenna elements is evaluated by the ECC and it is noted to be below 0.01. Furthermore, the SAR value does not exceed 0.288 W/Kg for an average mass of 10 g, and the radiation efficiency falls within the range of 70-90%. The effect of the user's hand was also studied and the obtained results showed that the user may affect the reflection coefficient of some antennas that are in contact with their hand, but the impedance matching and performance are still guaranteed. Several MIMO factors are also investigated and found to be good results.

ACKNOWLEDGEMENTS

We would particularly like to thank the Engineering Research Laboratory (LRI. Lab) at the Hassan II University of Casablanca for its substantial scientific support, and the journal staff for their constructive and helpful comments, which helped to improve the paper's quality.

REFERENCES

[1] K. S. Muttair, A. Z. G. Zahid, O. A. Shareef, A. M. Q. Kamil, and M. F. Mosleh, "A novel design of wide and multi-bands 2×2 multiple-input multiple-output antenna for 5G mm-wave applications," *International Journal of Electrical and Computer Engineering (IJECE)*, vol. 12, no. 4, pp. 3882–3890, Aug. 2022, doi: 10.11591/ijece.v12i4.pp3882-3890.

[2] S. Naik and A. Chari, "Design of a Multiband Microstrip Patch Antenna for 4G Application," in *Proc. IEEE International Conference for Innovation in Technology (INOCON)*, Bengaluru, India, 2020, pp. 1-4, doi: 10.1109/INOCON50539.2020.9298249.

[3] H. Zou, Y. Li, C. Y. D. Sim, and G. Yang, "Design of 8×8 dual-band MIMO antenna array for 5G smartphone applications," *International Journal of RF and Microwave Computer-Aided Engineering*, vol. 28, no. 9, p. e21420, Nov. 2018, doi: 10.1002/MMCE.21420.

[4] N. A. Bazadry, H. A. Rahim, M. N. M. Yasin, and M. Abdulmalek, "Quadruple band MIMO dielectric resonator antenna for 5G SUB-6 GHz applications," *Indonesian Journal of Electrical Engineering and Computer Science*, vol. 28, no. 3, 2022, pp. 1554-1562, doi: 10.11591/ijeecs.v28.i3.

[5] D. Rusdiyanto, D. W. Astuti, S. Alam, and Y. G. Adhiyoga, "Design of 2x2 Wide Bandwidth MIMO Antenna For LTE And 5G Sub-6GHz," *Journal of Informatics and Telecommunication Engineering*, vol. 5, no. 2, pp. 225–238, Jan. 2022, doi: 10.31289/JITE.V5I2.5699.

[6] Y. Liu, A. Ren, H. Liu, H. Wang, and C. Y. D. Sim, "Eight port MIMO array using characteristic mode theory for 5G-smartphone applications," *IEEE Access*, vol. 7, pp. 45679–45692, 2019, doi: 10.1109/ACCESS.2019.2909070.

[7] D. P. Mishra, K. K. Rout, and S. R. Salkuti, "Compact MIMO antenna using dual-band for fifth-generation mobile communication system," *Indonesian Journal of Electrical Engineering and Computer Science*, vol. 24, no. 2, pp. 921-929, 2021, doi: 10.11591/ijeecs.v24.i2.pp921-929.

[8] H. M. R. Nurul, Z. Mansor, and M. K. A. Rahim, "Dual element MIMO planar inverted-F antenna for 5G millimeter wave application," *TELKOMNIKA*, vol. 17, no. 4, pp. 1648-1655, Aug. 2019, doi: 10.12928/TELKOMNIKA.v17i4.12762.

[9] C. Zhang *et al.*, "A Dual Band Eight Element MIMO-Antenna Array for Future Ultrathin Mobile Terminals," *Micromachines*, vol. 13, no. 8, pp. 1267, Aug. 2022, doi: 10.3390/MI13081267.

[10] J. Huang, Z. Chen, Q. Cai, T. H. Loh, and G. Liu, "Minimized Triple-Band Eight-Element Antenna Array for 5G Metal-frame Smartphone Applications," *Micromachines*, vol. 13, no. 1, pp. 136, Jan. 2022, doi: 10.3390/MI13010136.

[11] K. Naveed, J. Nasir, and I. Khan, "Four-Element 8-Port *Dual*-band MIMO Antenna System for 5G Mobile Communication, " in *Proc. 16th International Conference on Emerging Technologies (ICET)*, Islamabad, Pakistan, 2021, pp. 1-5, doi: 10.1109/ICET54505.2021.9689789.
[12] D. Serghiou, M. Khalily, V. Singh, A. Araghi, and R. Tafazolli, "Sub-6 GHz dual-band 8×8 MIMO antenna for 5G smartphones," *IEEE Antennas Wirel Propag Lett*, vol. 19, no. 9, pp. 1546–1550, Sep. 2020, doi: 10.1109/LAWP.2020.3008962.
[13] M. Bridges, M. Khalily, M. Abedian, D. Serghiou, P. Xiao, and R. Tafazolli, "High Isolation 88 MIMO Antenna Design for 5G Sub-6 GHz Smartphone Applications," in *Proc. International Conference on UK-China Emerging Technologies (UCET)*, Aug. 2020, pp. 1-4, doi: 10.1109/UCET51115.2020.9205450.
[14] A. Ennajih, B. Nasiri, J. Zbitou, A. Errkik, and M. Latrach, "A wearable UHF RFID tag antenna-based metamaterial for biomedical applications," *Bulletin of Electrical Engineering and Informatics*, vol. 9, no. 2, pp. 676–684, Apr. 2020, doi: 10.11591/eei.v9i2.1661.
[15] M. Daghari and H. Sakli, "Radiation performance enhancement of an ultra wide band antenna using metamaterial band-pass filter," *International Journal of Electrical and Computer Engineering (IJECE)*, vol. 10, no. 6, pp. 5861–5870, Dec. 2020, doi: 10.11591/ijece.v10i6.pp5861-5870.
[16] A. Ennajih, B. Nasiri, J. Zbitou, A. Errkik, and M. Latrach, "A novel design of miniaturized tag antenna loaded metamaterial spiral split ring resonator," *International Journal of Intelligent Engineering and Systems*, vol. 12, no. 2, pp. 12-21, 2019, doi: 10.22266/IJIES2019.0430.02.
[17] E. Stavrou, O. Litschke, R. Baggen and C. Oikonomopoulos-Zachos, "Dual-beam antenna for MIMO WiFi base stations, " in *Proc. The 8th European Conference on Antennas and Propagation (EuCAP 2014)*, The Hague, Netherlands, 2014, pp. 1869-1871, doi: 10.1109/EuCAP.2014.6902160.
[18] M. S. Sharawi, A. T. Hassan, and M. U. Khan, "Correlation coefficient calculations for MIMO antenna systems: a comparative study," *Int J Microw Wirel Technol*, vol. 9, no. 10, pp. 1991–2004, Dec. 2017, doi: 10.1017/S1759078717000903.
[19] A. Kumar, "Compact 4x4 CPW-Fed MIMO Antenna with Wi-Fi and WLAN Notch for UWB Applications," *Radioelectronics and Communications Systems*, vol. 64, no. 2, pp. 92–98, 2021, doi: 10.3103/S0735272721020047.
[20] A. Khabba *et al*., "A new miniaturized wideband self-isolated two-port MIMO antenna for 5G millimeter-wave applications," *TELKOMNIKA (Telecommunication Computing Electronics and Control)*, vol. 21, no. 3, pp. 630-640, Jun. 2023, doi: 10.12928/TELKOMNIKA.v21i3.24139.
[21] E. Milshteyn *et al*., "Individualized SAR calculations using computer vision-based MR segmentation and a fast electromagnetic solver," *Magn Reson Med*., vol. 85, no. 1, pp. 429- 443, 2021, doi: 10.1002/mrm.28398.
[22] G. Srihari, R. Raman, S. Thangavelu, and N. Padmaja, "Hammer-shaped slotted antenna design and analysis for wireless applications," *Indonesian Journal of Electrical Engineering and Computer Science*, vol. 30, no. 3, pp. 1488-1497, Jun. 2023, doi: 10.11591/ijeecs.v30.i3.pp1488-1497.
[23] N. O. Parchin, H. J. Basherlou, Y. I. A. Al-yasir, A. M. Abdulkhaleq, M. Patwary, and R. A. Abd-Alhameed, "A New CPW-Fed Diversity Antenna for MIMO 5G Smartphones," *Electronics*, vol. 9, no. 2, pp. 261, Feb. 2020, doi: 10.3390/ELECTRONICS9020261.
[24] M. Abdullah *et al*., "High-performance multiple-input multiple-output antenna system for 5g mobile terminals," *Electronics (Switzerland)*, vol. 8, no. 10, pp. 1-16, Oct. 2019, doi: 10.3390/ELECTRONICS8101090.
[25] S. Nithya and V. Seethalakshmi, "MIMO Antenna with Isolation Enrichment for 5G Mobile Information," *Mobile Information Systems*, vol. 2022, pp. 1-14, 2022, doi: 10.1155/2022/1802352.
[26] S. I. Naqvi *et al*., "Integrated LTE and Millimeter-Wave 5G MIMO Antenna System for 4G/5G Wireless Terminals," *Sensors*, vol. 20, no. 14, p. 3926, Jul. 2020, doi: 10.3390/S20143926.
[27] M. Ikram, R. Hussain, and M. S. Sharawi, "4G/5G antenna system with dual function planar connected array," *IET Microwaves, Antennas & Propagation*, vol. 11, no. 12, pp. 1760–1764, Sep. 2017, doi: 10.1049/IET-MAP.2017.0148.
[28] J. Li *et al*., "Dual-Band Eight-Antenna Array Design for MIMO Applications in 5G Mobile Terminals," *IEEE Access*, vol. 7, pp. 71636–71644, 2019, doi: 10.1109/ACCESS.2019.2908969.
[29] N. Jaglan, S. D. Gupta, and M. S. Sharawi, "18 Element Massive MIMO/Diversity 5G Smartphones Antenna Design for Sub-6 GHz LTE Bands 42/43 Applications," *IEEE Open Journal of Antennas and Propagation*, vol. 2, pp. 533–545, 2021, doi: 10.1109/OJAP.2021.3074290.

BIOGRAPHIES OF AUTHORS

Abdelhadi Ennajih was born in octobre 1987 in Settat, Morocco. He received the State Engineer Diploma in Electrical Engineering from The National School of Applied Sciences of Tangier in 2012, later he received his Ph.D. degree in Electronics and Telecommunications from The Faculty of Science and Technology, Hassan I University, Settat, Morocco in 2018. He is currently Professor of Electronics and Telecommunications at the National Higher School of Electricity and Mechanics (ENSEM), Hassan II University, Casablanca, Morocco. He is involved of various radion frequency communication hardware design, metamaterial, RFID tag, and antennas development. He can be contacted at email: a.ennajih@ensem.ac.ma.

Azzeddine Sardi received a Ph.D. degree in Electronics and Telecommunications at The Faculty of Science and Technology of Settat, Hassan I University, Morocco, in 2017. His research interests include the analysis and design of the micro-wave power dividers, power combiners, couplers, and power limiters. He can be contacted at email: azzeddine.sardi@gmail.com.

Youssef Mouzouna received a Ph.D. in Electronics and Telecommunication from the Hassan I University in 2019. He is currently an Assitant Professor at The Department of Electrical Engineering at the National Higher School of Electricity and Mechanics (ENSEM). His current research interests include RFID systems, embedded systems, blockchain, and the internet of things. He can be contacted at email: y.mouzouna@ensem.ac.ma.

Mohamed Sadik received his Ph.D. degree from the National Polytechnic Institue of Lorraine (INPL) (Nancy, France) in Electrical Engineering in 1992. He is currently a full Professor at the Department of Electrical Engineering at the National School of Electrical and Mechanical Engineering (ENSEM). He was chair of the Department of Electrical Engineering (2008-2013) and was chair of the Research and cooperation department at ENSEM from 2013 to 2019. He has founded and led the Networks, Embedded Systems and Telecom (NEST Reasearch Group component if LRI lab.) (2011-2020). Now he is Director of the Laboratory of Research in Engineering (LRI Lab.). He served on the technical program committees of many international conferences (and as a reviewer of several journals). Pr. Sadik has co-founded the International Symposium on Ubiquitous Networking (UNet) and serves as TPC chair and general Chair of some conferences. He can be contacted at email: m.sadik@ensem.ac.ma.

Ahmed Errkik received was born in Morocco in 1960. He received a Ph.D. degree from The University of Technology Compiègne (UTC), Compiègne, France in Physics. He is currently Professor of Physics at The Faculty of Science and Technology, University Hassan I, Settat, Morocco, and he is the Head of the Laboratory LMIET. He is involved in the design of hybrid, monolithic active, and passive microwave electronic circuits. He can be contacted at email: ahmed.errkik@uhp.ac.ma.